Indian Journal of Chemical Technology
Vol. 31, July 2024, pp. 622-630
DOI: 10.56042/ijct.v31i4. 8734

Efficient organic-MgO matrix as adsorbent for heavy metal uptake: Spectroscopic, adsorption isotherms, kinetic and thermodynamic analysis

Naresh Kumar Sharma[1], Jyotsna Ratan[2], Namita Gandhi[3], Sajid Ali[4] & Atul Kumar Srivastava[5]*

[1]Department of Chemistry, Government P.G. College, Bundi-323001, India

[2]Department of Chemistry, Zakir Husain Delhi College, University of Delhi, New Delhi-110002, India

[3]Department of Chemistry, Deshbandhu College, University of Delhi, New Delhi-110019, India

[4]Department of Chemistry, Maulana Azad National Urdu University Polytechnic, Bangalore-560072, India

[5]P.G. Department of Chemistry, Magadh University, Bodh Gaya-824234, India

*E-mail: dratulk2019@rediffmail.com

Received 12 February 2024; accepted 26 April 2024

In this study, a new adsorbent has been developed by modifying a low-cost and readily available waste, namely the dried orange (*Citrus aurantium* Linn) peel (CiR). The removal of heavy metals pollutants by binding of magnesium oxides (MgO) on the peel represents a simple, economical, and faster method. Various analysis, including X-ray diffraction, Fourier transforms infrared spectroscopy and application of mathematical models, have been performed on the modified adsorbent (dried *Citrus reticulata* peel + MgO; CiR-MgO matrix). The abundant free functional groups present in the biomass and metal oxides collectively exert interactive forces leading to the sorption of Zn^{2+} heavy metals. The Langmuir isotherm and pseudo-first order kinetic models are confirmed as the best fitted model of the adsorption process through chi-analysis. The rate-limiting step of intra-particle diffusion governs the adsorption process. This method is best suited for fixed-bed column application due to its fast kinetics, hydrophilic nature, and regeneration process with 0.005 M HCl.

Keywords: Agricultural waste, *Citrus aurantium* Linn, Heavy metals, Low-cost adsorbents, Organic-metal matrix

Introduction

Till date, industrial and municipal wastewater treatment has gained enormous attention due to its direct interaction with the biosphere. The presence of heavy metals in wastewater poses critical health concern. Heavy metals, such as mercury, cadmium, lead, chromium, arsenic, zinc, copper, nickel, cobalt among other, are non-biodegradable, bioaccumulated and can leads to cancer[1-5]. Thus, heavy metal concentrations above critical limits could be harmful to living organisms. Zinc, an essential trace element, may become harmful at elevated concentration, cause disturbances in energy metabolism and increase the oxidative stress[6].

Various methods have been proposed for removing heavy metal pollutant, including ion exchange, co-precipitation, adsorption, membrane filtration, precipitation, and treatments based on photocatalyst[7, 8]. However, adsorption is found to be superior in terms of effectiveness, economy, simplicity, ease of operation and the regeneration of adsorbent[9]. Hence, metal oxides have also been employed to exclude heavy metals from contaminated wastewater[10,11]. Through physical sorption or chemical impregnation, metal oxides surfaces can retain heavy metals[12]. Polymeric extractants[13] involves unwieldy synthesis and purification procedures as well as high cost. Therefore, agricultural waste and/or by products have gained much attention as adsorbent. However, the presence of diverse hazardous chemicals demands more effectiveness in heavy metals adsorption. Thus, it was deemed worthwhile to develop a new adsorbent by modifying a low-cost and highly available waste product of an agro-based product through a simple and convenient process of *in-situ* oxidation cum deposition of metal oxide with hydrogen peroxide. This oxidation process results in an increase in active sites due to the formation of new additional functional groups after the degradation of larger and/ or polymeric molecules[14]. Consequently, simple and fast procedures for the modification agricultural products have been pursued to obtain effective adsorbents that exhibit sequestering behavior similar to naturally occurring soil constituents (metal oxides-organic matrix). The species and biomass origin used as adsorbent govern the qualitative and quantitative mechanisms of the metals adsorption[15].

The Mandarin orange (*Citrus reticulata*), belonging to the family Rutaceae is a delectable and ubiquitous fruit. Its production amount to about 29 million tons, ranking 9th among major fruit crops, and occurs mostly in tropical and subtropical regions of the world[16]. A mandarin orange contains 85% water, 13% carbohydrates, and negligible amounts of fat and protein[17]. Among micronutrients, only vitamin C is in significant content (32% of the Daily Value) in a 100 g reference serving, with all other nutrients in low amounts[18]. Various pharmacological activities have been exhibited by the extract of CiR, such as antioxidant[19], anti-inflammatory and anti-nociceptive agents[20], antibacterial activity[21] and anticancer activity[22]. MgO-based materials are known to remove heavy metals, for example, MgO-SiO_2 has been reported to remove Cu^{2+}, Ni^{2+} and Zn^{2+} ions[23] and MgO/palygorskite for the removal of Cd^{2+} and Zn^{2+} (Ref.24).

No apparent study has revealed magnesium oxides binding on biomass through simple and fast *in-situ* oxidation with hydrogen peroxide. Hence, the present work was carried out to determine the potential of the new sorbent formed by magnesium oxides binding with the CiR peel for heavy metal elimination from wastewater. In this work, wasted CiR peel has been modified by adding MgO. The present study can propose new insights into the mechanism of the adsorbent and possible new series of adsorbents.

Experimental Section

Materials and Method

Zinc sulphate (Loba Chemie Pvt. Ltd., India), magnesium nitrate (Panreac Quimica S.A., Spain) and hydrogen peroxide (20%) solution (Sigma Aldrich Chemie GmbH, Germany) were employed. All reagents were of analytical grade. Oranges (*Citrus aurantium* Linn) were sourced from the Delhi local fruit market and their peels were collected for the study.

Buffers were prepared as follows: pH 1-2 (0.2 M KCl in 0.2 M HCl), pH 3-5 (0.1 M CH_3COOH in 0.1 M CH_3COONa), pH 6 (1.0 M CH_3COOH + 1.0 M NaOH) and pH 8-10 (NH_4Cl + NH_4OH) [25,26].

Flame atomic absorption spectrometry (Agilent, USA), a pH meter (GOnDO Electronic Co. Ltd., Taiwan), a magnetic stirrer (Benchmark Scientific, USA) and ASTM standard sieves were utilized in the experiment.

Adsorbent synthesis

Approximately 50 g of dried, grounded orange (*Citrus aurantium* Linn) peel (CiR) was mixed with 50 mL of Mg^{2+} (0.1 M) in a 500 mL beaker equipped with a magnetic rod. Hydrogen peroxide was added to the solution until no changes/reaction were observed, with constant stirring. The reaction mixture was then left to age for 2 days at room temperature. The obtained solid product (light cream) was filtered using a suction pump, then dried in an oven at 70°C until a constant weight was achieved.

Water regain capacity and hydrogen capacity procedure

The adsorbent (0.1 g) was soaked in dd. H_2O for two days, filtered, air-dried, and then dried overnight at 70°C.

The water regain capacity (W) was calculated using the formula[27]:

$$W = \frac{(m_w - m_d)}{m_d}$$

For hydrogen capacity, the adsorbent (0.1 g) was soaked in HCl solution (4 M) for 1 h, filtered, washed with distilled water until no free acid leached, and dried at 60°C for 3 h. The dried acidified adsorbent was then added to NaOH solution (0.1 M) and allowed to age for one hour to reach equilibrium. The residual alkali was titrated against HCl (0.1 M).

Method for single batch

An appropriate buffer was used to maintain a constant pH of a solution containing Zn^{2+} ions in contact with a precisely weight adsorbent. The mixture was stirred continuously for a pre-selected period, after which the filtrate containing Zn^{2+} ion was analyzed using flame atomic absorption spectrometry. The adsorption capacity at equilibrium (q_e) was calculated using the formula:

$$q_e = (C_o - C_e) \times \frac{V}{W}$$

where, q_e corresponds to adsorption capacity at equilibrium (mg g^{-1}), C_0 to the initial concentration (mg L^{-1}), C_e corresponds the equilibrium concentration (mg L^{-1}), V represents the solution volume and w is the adsorbent weight (g).

Results and Discussion

Characterizations

The properties of the metal oxide surface are typically altered due to heavy metal adsorption, necessitating a comprehensive study of the end product for better understanding of the sorption mechanism[28].

FTIR spectroscopy

The presence of the band of ν(MgO) at 872 cm^{-1} indicates the anchoring of MgO onto the organic support (CiR)[29]. Loading of Zn^{2+} resulted in additional peaks at 429, 588 and 781 cm^{-1} (corresponding to νZnO)[29, 30]. A shift in the band from 1647-1651 cm^{-1} suggests the involvement of C=O in maintaining Zn^{2+} (Fig. 1). Peaks of C=O at 1771 cm $^{-1}$ disappeared from the spectrum after loading with Zn^{2+}, indicated its role in retaining Zn^{2+}. New peaks at 3487 and 3674 cm^{-1} were assigned to certain groups being reduce to OH due to ammonia. These observations suggest that both the organic functional groups of CiR and MgO contribute to altering the overall adsorption capacity for Zn^{2+}.

X-ray Diffraction (XRD) and X-ray Fluorescence (XRF) studies

The XRD pattern (Fig. 2) of the developed adsorbent lacked sharp peaks, indicated its amorphous nature due to the composition of a mixture of organic (CiR) and inorganic (MgO) materials. The appearance of a peak, at 2θ= 38.78°, corresponding to the (111) plane of MgO[31], confirms the successfully incorporation of magnesium oxide onto the biomass. XRF analysis confirmed the composition of the adsorbent as 19.20% MgO, along with major components such as S (24.49%), SiO_2 (10.80%), and C (20.19%).

Effect of pH

To assess the adsorption properties of CiR-MgO for Zn^{2+} onto its surface, several batches of different pH were prepared. About 0.1 g of the adsorbent was mixed in 1 x 10^{-2} (M) Zn^{2+} solution to prepare the suspension of each batch, with pH maintained at a constant value by using an appropriate buffer.

Fig. 3 illustrates that the metal oxide surface charge is affected by the pH of the solution, thereby influencing CiR-MgO adsorption efficiency. The amount of surface charge is reflected by the hydrogen ion capacity value, observed at 2.8 mmol g^{-1}. Lower

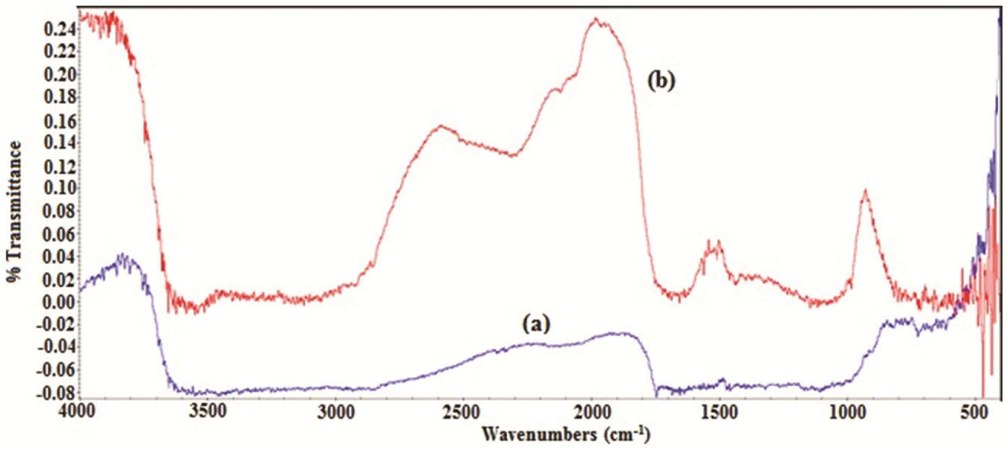

Fig. 1 — FTIR spectra of CiR-MgO Matrix (a) before and (b) after loading with the analyte (Zn^{2+})

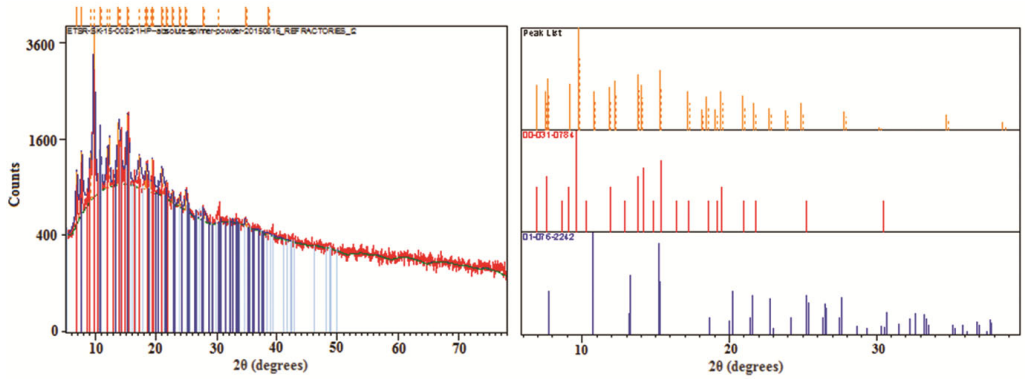

Fig. 2 — X-ray diffractograms of the adsorbent affirming the incorporation of MgO onto the organic matrix

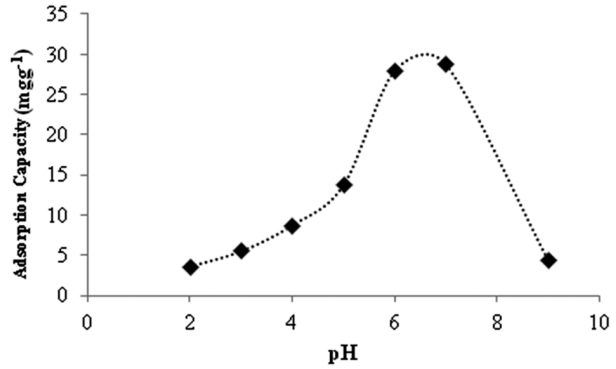

Fig. 3 — Adsorption capacity on the CiR-MgO Matrix at various pH

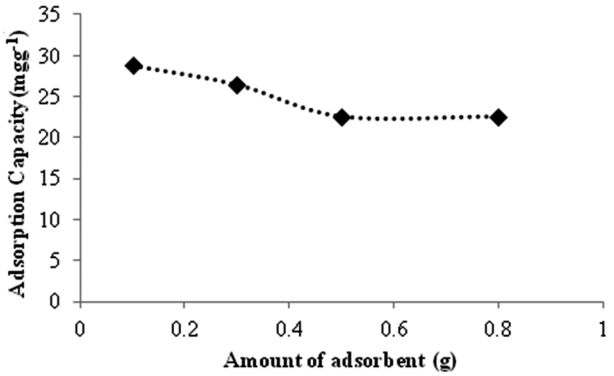

Fig. 4 — Adsorption capacity of Zn^{2+} at various amount of CiR-MgO Matrix

adsorption capacity at pH < 5.0 indicate that the protonated surface becomes positively charged, and exhibiting lower affinity for Zn^{2+} due to electrostatic repulsion. However, at pH > 5, there is a steady increase in Zn^{2+} uptake, ultimately reaching the highest adsorption efficiency at pH 7. The pH-dependent nature of the adsorption capacity suggested that the surface of MgO bears replaceable hydrogen either as MgO(OH) or $Mg(OH)_2$ or both together.

The tendency of the metal oxide surface to attain a hydroxyl group is reflected in its water-regaining capacity[32]. Similar results were observed for CiR-MgO, indicating the hydrophilic character of the prepared adsorbent. The hydrophilicity of the adsorbent facilitates inter-phase and intra-phase transport of Zn^{2+} between the solid adsorbent and the solution, leading to better adsorption[32]. The observed water regains capacity of the prepared adsorbent was 2.8 g per unit (g).

Effect of amount of adsorbent

Several batches containing varying amounts of the adsorbent were prepared. Each batch consisted of a suspension of 5.0×10^{-5} M Zn^{2+} solution with a specific quantity of adsorbent. Optimum pH was maintained for all the batches. The maximum adsorption capacity was attained with 0.1 g (Fig. 4) of the adsorbent, providing an optimal surface area. However, increasing the amount of adsorbent beyond 0.1 g did not significantly alter the adsorption capacity. This lack of change may be attributed to the non-availability of additional free adsorption sites on the adsorbent surface, suggesting that electrostatic forces on the Zn^{2+} ions-laden surface are not favorable for further adsorption.

Effect of concentration

Multiple batches were prepared to assess the effect of concentration. Each batch consisted of 0.1 g of CiR-MgO suspended in varying concentrations (5.0×10^{-6} – 25.0×10^{-6} M) of Zn^{2+} solutions. Optimum pH was maintained for these suspensions by continuously stirring for 1 h. As initial concentration of Zn^{2+} ions in direct contact with the CiR-MgO surface increased, adsorption also increase. This suggests that vacant sites are available until saturation at about 25.0×10^{-6} mol L^{-1} of Zn^{2+} concentration, indicating a linear relationship between Zn^{2+} concentration and available free sites up to saturation.

K_d, the partition ratio, also known as the distribution ratio, is a measure that reflects adsorbent's affinity for the metal ions[33]. It is the ratio of adsorbent's adsorption capacity to the residual concentration metal ions (such as Zn^{2+}) in the solution. The K_d can be represented as:

$$K_d = \frac{q}{c}$$

where c represents the Zn^{2+} concentration remaining in the solution, and q represents the Zn^{2+} adsorbed on the CiR-MgO matrix. The prepared CiR-MgO matrix for Zn^{2+} exhibited high affinity, with a partition ratio of 3.2.

Effect of contact time

To determine the adsorption of Zn^{2+} over varying durations, several batches with a constant optimum pH and 0.1 g of CiR-MgO matrix suspended in 5.0×10^{-5} M Zn^{2+} solution were prepared. A minimum contact time of 20 min was required to achieve the highest adsorption capacity, approximately 28.80 mg g^{-1}. The rapid kinetics reaffirmed the strong affinity of the adsorbent towards Zn^{2+}. This favorable nature may have resulted from the hydrophilicity of the adsorbent.

Surface charge and pH_{PZC}

A salt titration method, as previously reported[34], was employed to determine the pH at pH_{PZC} (zero surface charge density). During titration, the increase in surface charge density altered the pH of the Zn^{2+} solution, which ultimately stabilized at pH_{PZC}. Davis & Leckie[34] observed that the total number of available surface protons reflects the surface charge density, a parameter easily measurable through potentiometric titration.

The presence of hydroxyl group accounts for the surface charge of metal-based adsorbents[35]. The value of pH_{PZC} reflects the surface charge of the metal oxide. The MgO surface becomes protonated at pH 5, providing a positive surface charge. However, the sorption of cations is favoured as surface sites becomes deprotonated ($pH > pH_{PZC}$).

Kinetic study

Understanding the effect, mechanism, and rate of Zn^{2+} adsorption on the CiR-MgO matrix is crucial. Therefore, selecting the most appropriate kinetic model is essential for analyzing the adsorption rate order. As reported, if q_1 and q_t represent the amount (mg g^{-1}) of the Zn^{2+} ion adsorbed at time t when the equilibrium point is reached, and k_1 represents the pseudo-first-order rate constant (min^{-1}) in the kinetic model equation for adsorption, it is expressed as follows[36]:

$$\frac{1}{q_t} = \frac{1}{q_1} + \frac{K_1}{q_1 t}$$

A correlation coefficient of 0.98 suggested a pseudo-first-order rate. There was minimal difference observed when comparison the adsorption capacity obtained from the pseudo-first-order model with experimental result, supporting its suitability. The positive rate constant indicates its appropriateness. If q_2 and q_t denote the amount (mg g^{-1}) of Zn^{2+} ion adsorbed at time t when the equilibrium point is reached, and K_2 represents the pseudo-second-order rate constant in the kinetic model equation for adsorption, it is expressed as follow [36]:

$$\frac{1}{q_t} = \frac{1}{K_2 q_2^2} + \frac{1}{q_2} t$$

A correlation coefficient of 0.97 suggested a pseudo-second-order rate. However, a significant difference was observed when comparing the theoretically obtained adsorption capacity with experimental results, indicating the unsuitability of the model.

Diffusion study

The surface of the adsorbent may exert a diffusion barrier against the approaching Zn^{2+}, migrating from the bulk solution towards the adsorbent surface[37]. The rate of adsorption of Zn^{2+} is influenced by (i) external diffusion (ii) internal diffusion, or (iii) collectively external and internal diffusion. The migration of Zn^{2+} from the bulk of the solution towards the boundary layer of the liquid phase is governed by external diffusion. Conversely, the movement of Zn^{2+} from the external surface to the pores of the internal surface of the adsorbent is governed by internal diffusion[38].

According to the external mass transfer diffusion model, intraparticle diffusion can be ignored initially, assuming negligible surface concentration of Zn^{2+} at time (t) = 0 (Ref.39). The external mass transfer coefficient, k_f, and the rate at which the residual concentration of Zn^{2+} changes are correlated as:

$$\frac{dC_t}{dt} = -K_f A(C_t - C_s) \qquad C_t = C_0 \text{ at } t = 0$$

where, C_t represents the residual concentration of Zn^{2+} at time (t), and C_s represents the residual concentration of Zn^{2+} at the surface. The surface area for mass transfer[40] is represented by A. Therefore, if a linear relationship is represented by a plot of ln C_t against C_0 time t, then it would indicate that the adsorption kinetics is quite dependent on the rate of the reaction occurring on the surface[41,42]. The intraparticle[43] can be expressed as follows:

$$q_t = k_p t^{1/2} + C$$

where, C is intercept and k_p is the intraparticle diffusion rate constant (mg g^{-1} $min^{-1/2}$).

The plot of q_t *vs.* $t^{1/2}$ reflects two stages, with the first stage representing external diffusion and the second stage representing internal diffusion[44,45]. The negligible boundary layer control, indicated by the intercept close to the origin, suggests intraparticle diffusion (Table 1) as the rate-limiting step[44,46].

The liquid film model[47], as represented by the expression:

$$\ln\left(1 - \frac{q_t}{q_e}\right) = -K_f dt$$

where, k_{fd} represents the adsorption rate coefficient expressed as min^{-1}, which would be valid and suitable for governing the adsorption process if the process prolongs the movement of Zn^{2+} from the

Table1 — Different parameter calculated when Zn^{2+} adsorbed on the CiR-MgO Matrix

Pseudo-first order constants		Pseudo-second order constants		Intraparticle diffusion constants	
$k_1(min^{-1})$	0.12	$k_2(g\ mg^{-1}\ min^{-1})$	2.8×10^{-4}	$k_p(mg\ g^{-1}\ min^{-1/2})$	7.39
q_{e1} (mgg^{-1})	34.27	q_{e2} (mgg^{-1})	37.04	$C(mg\ g^{-1})$	12.87
$r1^2$	0.98	$r2^2$	0.97	rp^2	0.96

Table 2 — Parameter calculated from different isotherm model when Zn^{2+} adsorbed on the CiR-MgO matrix

Langmuir's isotherm constants		Freundlich's isotherm constants	
R_L	0.83	n	1.65
$K_L(dm^3 mg^{-1})$	43.48	$K_F(dm^3\ mg^{-1})$	4.16
r^{2L}	0.99	r^{2F}	0.99

solution towards the adsorbent's surface.

Therefore, for the slowest stage of the adsorption process, a linear plot of $-\ln (1 - q_t/q_e)$ *versus* time would have a zero intercept. However, in the present study a very high intercept was observed and a low linearity curve was obtained for liquid film diffusion, thus ruling out the model.

Isotherm study

The adsorption isotherm, operating under constant temperature and pH conditions, dictates the migration of Zn^{2+} ions from an aqueous solution to a solid substrate. Both the derived physiochemical parameters and the underlying assumptions used to gauge the thermodynamics provide valuable insights into the adsorption mechanism, the level of affinity, and the surface characteristics of the adsorbent[48]. The mathematical formulations of the isotherm models offer a visual representation of the Zn^{2+} adsorption process involving the solid substrate and the residual concentration of the analyte[49-51].

Langmuir's isotherm model[50,51] describes chemisorption through monolayer adsorption. It posits the existence of a specific number of unoccupied sites with uniform energy and surface coverage, where there is no interaction among the Zn^{2+} ions on the CiR-MgO matrix.

The equation encapsulating the Langmuir isotherm can be represented as follows:

$$\frac{1}{q_e} = \frac{1}{q_{max}} + \left(\frac{1}{q_{max} K_L}\right)\frac{1}{C_e}$$

where q_e (mg g^{-1}) denotes the quantity of Zn^{2+} adsorbed at equilibrium, and C_e (mol dm^{-3}) signifies the residual concentration of Zn^{2+}. Furthermore, q_{max} (mg g^{-1}) represents the monolayer adsorption capacity, while K_L (dm^{-3} mg^{-1}), the Langmuir adsorption constant, is associated with the free adsorption energy. The affinity of Zn^{2+} can be assessed through the equilibrium parameter value, R_L, also known as the separation factor, which is linked to K_L as follows:

$$R = \frac{1}{1 + K_L C_0}$$

where C_0 represents the initial concentration of Zn^{2+}. A value of R_L less than unity indicates favourable adsorption, while a value greater than unity suggests unfavourable adsorption[51]. In this scenario, an R_L value less than unity reveals the favourable adsorption of Zn^{2+} onto the adsorbent (Table 2). The adsorption of Zn^{2+} occurs in a monolayer fashion, as indicated by a correlation coefficient of 0.99, as implied by Langmuir's isotherm. Swedlund & Webster[52] propose the existence of homogeneous active adsorption sites, facilitating physiochemical sorption through ion pairs or inner-sphere complexes.

Freundlich's isotherm model represents the heterogeneous and exponential distribution of energy and active sites. It predicts the phenomenon of physisorption through its assumption of infinite surface coverage[50,51]. The Freundlich isotherm can be represented as:

$$\log q_e = \log K_f + \frac{1}{n}\log C_e$$

where K_F (dm^3 g^{-1}) signifies the Freundlich adsorption capacity, and n is the constant representing the adsorption intensity.

The value of n denotes the degree of non-linearity in the relationship between solute concentrations and adsorption. As Zn^{2+} continues to occupy surface adsorption sites, a gradual decrease in adsorption is observed, possibly due to repulsive interactions (of ionic nature) between Zn^{2+} ions in the solution and the metallic ions adsorbed on the surface[53]. The obtained n value (1.65) suggests physical adsorption[54].

Multilayered adsorption is also evidenced by a correlation coefficient of 0.99. A value closer to unity indicates that active binding sites are heterogeneously distributed, leading to physiochemical sorption. The suitability of the isothermal models can be further assessed through Chi-analysis.

Error analysis

The coefficient of determination, represented by the r^2 value, obtained from Langmuir's and Freundlich's models, yielded inconclusive results regarding the best fit. Fortunately, the Chi-square test[55] can be utilized to ascertain the most suitable model. The Chi-square (χ^2) is typically defined as:

$$x^2 = \sum \frac{\left(q_e - q_{e,m}\right)^2}{q_{e,m}}$$

where $q_{e,m}$ represents the equilibrium capacities analyzed from the model, and q_e (mg/g) is obtained experimentally.

A small value of χ^2 indicates the most suitable model. The Langmuir isotherm and Freundlich's adsorption isotherm models yielded χ^2 values of 4.98 and 145.09, respectively. Therefore, the Langmuir isotherm model is considered the best-fitting adsorption model. Furthermore, when encountering similar correlation coefficient values for both the pseudo-first order and pseudo-second order, employing the Chi-square test can resolve the issue. The lower χ^2 value of 0.89 obtained for the pseudo-first order signifies a better fitting model compared to the χ^2 value of 1.85 obtained for the pseudo-second order model.

Regenerability

The significance of the current desorption study lies in its contribution to the recycling of adsorbents and the recovery of metal ions. The pH-dependent adsorption and desorption processes play a pivotal role in governing surface reactions of metal oxides. The percentage of analyte recovery was calculated as follows:

$$\text{Recovery (\%)} = \frac{\text{Amount of analyte desorbed}}{\text{Amount of analyte adsorbed}} \times 100$$

The acids studied, including HCl, HNO_3, and CH_3COOH, were investigated, and among them, HCl (0.005 M) resulted in approximately 100% recovery of the retained Zn^{2+}. Following the regeneration of the adsorbent, it was utilized for numerous elution-loading cycles. By 40th cycle, only an 8% loss in adsorption capacity was observed, likely attributed to the initial degradation of the organic component of the adsorbent.

Conclusion

In this study, we demonstrate the formation of a CiR-MgO matrix for the removal of heavy metal ions using waste from *Citrus aurantium* Linn (CiR) peel and MgO. This method not only utilizes waste but also serves as an effective treatment for wastewater. It offers a straightforward, cost-effective, and rapid solution for eliminating heavy metal pollutants. The successful removal of Zn^{2+} (used as a model for heavy metal pollutants) clearly indicates the potential of the new adsorbent as an efficient heavy metal scavenger. The adsorption process conforms to Langmuir's model, suggesting interactions of ion pairs or inner-sphere complexes with Zn^{2+} ions. The adsorption capacity is influenced by pH, indicating the presence of replaceable hydrogen in the form of MgO(OH) and $Mg(OH)_2$ on the surface of MgO. The optimal pH (pH = 7) for maximum adsorption suggests that the adsorbent could effectively target a wide range of heavy metals. At this pH, many heavy metals exhibit minimal tendency to precipitate as hydroxides. Furthermore, the simple preparation, enhanced adsorption capacity, rapid kinetics, near-neutral pH of adsorption, and ease of regeneration underscore its potential for widespread application in water treatment on a large scale. Additionally, a fixed bed column method can be employed with this highly hydrophilic adsorbent.

References

1 El-Sherif I Y, Tolani S, Ofosu K, Mohamed O A & Wanekaya A K, Polymeric nanofibers for the removal of Cr(III) from tannery waste water, *J Environ Manag*, 129 (2013) 410.

2 Zou Y, Wang X, Khan A, Wang P, Liu Y, Alsaedi A, Hayat T & Wang X, Environmental remediation and application of nanoscale zerovalent iron and its composites for the removal of heavy metal ions: A review, *Environ Sci Technol*, 50 (2016) 7290.

3 Diaper C, Tjandraatmadja G, Pollard C, Tusseau A C, Price G, Burch L, Gozukara Y, Sheedy C & Moglia M, Sources of critical contaminants in domestic wastewater: Contaminant contribution from household products, *Water Health Country Flag Rep Ser*, (2008).

4 Taseidifar M, Makavipour F, Pashley R M & Rahman A F M M, Removal of heavy metal ions from water using ion flotation, *Environ Technol Innov*, 8 (2017) 182.

5 García-Niño W R & Pedraza-Chaverrí J, Protective effect of curcumin against heavy metals-induced liver damage, *Food Chem Toxicol*, 69 (2014) 182.

6 Borba C E, Guirardello R, Silva E A, Veit M T & Tavares C R G, Removal of nickel(II) ions from aqueous solution by biosorption in a fixed bed column: Experimental and theoretical breakthrough curves, *Biochem Eng J*, 30 (2006) 184.

7 Shi P, Xiao J, Wang Y & Chen L, Assessment of ecological and human health risks of heavy metal contamination in agriculture soils disturbed by pipeline construction, *Int J Environ Res Public Health*, 11 (2014) 2504.

8 Laskar M A, Siddiqui S & Islam A, Reflection of the physiochemical characteristics of 1-(2-pyridylazo)-2-naphthol on the pre-concentration of trace heavy metals, *Crit Rev Anal Chem*, 46 (2016) 413.

9 Naef A A Q, Ramy H M & Dahiru U, Lawal removal of heavy metal ions from wastewater: A comprehensive and critical review, *NPJ Clean Water*, 4 (2021) 36.

10 Laskar M A, Ali S K & Siddiqui S, Characterization of the kinetics and thermodynamics for the adsorption of zinc(II) on fennel seeds, *Anal Lett*, 49 (2016) 1537.

11 Fan M, Boonfueng T, Xu Y, Axe L & Tyson T A, Modeling Pb sorption to microporous amorphous oxides as discrete particles and coatings, *J Colloid Interface Sci*, 281 (2005) 39.

12 Hua M, Zhang S, Pan B, Zhang W, Lv L & Zhang Q, Heavy metal removal from water/wastewater by nanosized metal oxides: A review, *J Hazard Mater*, 211 (2012) 317.

13 Martin T A & Kempton J H, In situ stabilization of metal-contaminated groundwater by hydrous ferric oxide: An experimental and modeling investigation, *Environ Sci Technol*, 34 (2000) 3229.

14 Ahmad A, Siddique J A, Laskar M A, Kumar R, Mohd-Setapar S H, Khatoon A & Shiekh R A, New generation Amberlite XAD resin for the removal of metal ions, *J Environ Sci*, 31 (2015) 104.

15 Barbusinski K, Fenton reaction-controversy concerning the chemistry, *Ecol Chem Eng*, 16 (2009) 247.

16 Goldenberg L, Yaniv Y, Porat R & Carmi N, Mandarin fruit quality: A review, *J Sci Food Agric*, 98 (2018) 18.

17 Viuda-Martos M, Ruiz-Navajas M, Fernández-López J, Pérez-Álvarez I & José A, Chemical composition of mandarin (*C. reticulata* L.), Grapefruit (*C. paradisi* L.), Lemon (*C. limon* L.) and Orange (*C. sinensis* L.) Essential Oils, *J Essent Oil Bearing Plants*, 9 (2009) 236.

18 German Nutrition Society (DGE), New Reference Values for Vitamin C Intake, *Ann Nutr Metab*, 67 (2015) 13.

19 Tumbas V T, Ćetković G S, Djilas S M, Čanadanović-Brunet J M, Vulić J J, Knez Ž & Škerget M, Antioxidant activity of mandarin (Citrus reticulata) peel, *Acta Period Technol*, 41 (2010) 195.

20 Malleshappa P, Kumaran R C, Venkatarangaiah K & Parveen S, Peels of citrus fruits: A potential source of anti-inflammatory and anti-nociceptive agents, *Pharmacogn J*, 10 (2018) 172.

21 Song X, Liu T, Wang L, Liu L, Li X & Wu X, Antibacterial effects and mechanism of mandarin (Citrus reticulata L.) essential oil against staphylococcus aureus, molecules, 25 (2020) 4956.

22 Cirmi S, Maugeri A, Ferlazzo N, Gangemi S, Calapai G, Schumacher U & Navarra M, Anticancer potential of *Citrus* Juices and their extracts: A systematic review of both preclinical and clinical studies, *Front Pharmacol*, 8 (2017) 420.

23 Ciesielczyk F, Damian A, Krenc A & Jesionowski T, MgO-SiO_2 inorganic oxide system as an adsorbent of heavy metais, *Przem Chem*, 91 (2012) 713.

24 Tian G, Wang W, Zong L & Wang A, MgO/palygorskite adsorbent derived from natural Mg-rich brine and palygorskite for high-efficient removal of Cd(II) and Zn(II) ions, *J Environ Chem Eng*, 5 (2017) 1027.

25 German W L & Vogel A I, A new series of buffer mixtures covering the pH range 1-6, *Analyst*, 62 (1937) 271.

26 Lurie Y Y, *Hand book of Analytical Chemistry*, Moscow: MIR Publishers, (1975).

27 Islam A, Laskar M A & Ahmad A, Characterization of a novel chelating resin of enhanced hydrophilicity and its analytical utility for preconcentration of trace metal ions, *Talanta*, 81 (2010) 1772.

28 Stumm W & Morgan J J, *Aquatic Chemistry*, New York: John Wiley & Sons, (1996).

29 Miller F A & Wilkins C H, Infrared spectra and characteristic frequencies of inorganic ions, *Anal Chem*, 24 (1952) 1253.

30 Coates J, *Encyclopedia of Analytical Chemistry*, Meyers, R A, Eds, Chichester**:** John Wiley & Sons Ltd, (2000).

31 Hubbard C R, *Standard X-ray Diffraction Powder Patterns*, Washington: International Centre for Diffraction Data, National Measurement Laboratory, National Bureau of Standards, (1981).

32 Islam A, Laskar M A & Ahmad A, Preconcentration of metal ions through chelation on a synthesized resin containing O, O donor atoms for quantitative analysis of environmental and biological samples, *Environ Monit Assess*, 185 (2013) 2691.

33 Siddiqui S, Otaif K & Laskar M A, Characterization and efficacy of a new generation scavenger of heavy metal pollutant: A green method of remediation of wastewater, *Int J Environ Sci Technol*, 13 (2016) 2951.

34 Davis J A & Leckie J O, Surface ionization and complexation at the oxide/water interface II. Surface properties of amorphous iron oxyhydroxide and adsorption of metal ions, *J Colloid Interface Sci*, 67 (1978) 90.

35 Karatapanis A E, Petrakis D E & Stalikas C D, A layered magnetic iron/iron oxide nanoscavenger for the analytical enrichment of ng-L−1 concentration levels of heavy metals from water, *Anal Chim Acta*, 726 (2012) 22.

36 Laskar M A, Ali S K & Siddiqui S, The remediation of wastewater by adsorption on an agro-based waste, *Indian J Environ Prot*, 6 (2016) 81.

37 Gupta V K, Mittal A & Gajbe V J, Adsorption and desorption studies of a water soluble dye, quinoline yellow, using waste materials, *Colloid Interface Sci*, 284 (2005) 89.

38 Gupta V K, Ali I, Suhas & Mohan D, Equilibrium uptake and sorption dynamics for the removal of a basic dye (basic red) using low cost adsorbents, *J Colloid Interface Sci*, 265 (2003) 257.

39 Sag Y & Aktay Y, Mass transfer and equilibrium studies for the sorption of chromium onto chitin, *Process Biochem*, 36 (2000) 157.

40 Guiza S & Bagane M, Equilibrium studies for the adsorption of dyes on natural clay, *Ann Chim Sci Mat*, 29 (2004) 615.

41 Spahn H & Schlunder E U, The scale-up of activated carbon columns for water purification, based on results from batch tests-I: Theoretical and experimental determination of adsorption rates of single organic solutes in batch tests, *Chem Eng Sci*, 30 (1975) 529.

42 Jin Y, Wu Y, Cao J & Wu Y, Adsorption behavior of Cr(VI), Ni(II), and Co(II) onto zeolite 13x, *Desalin Water Treat*, 54 (2015) 511.

43 Weber J W J, Morris J C & Sanit J, Kinetics of adsorption on carbon from solution, *J Sanit Eng Div Am Soc Civil Eng*, 89 (1963) 31.

44 Ma X, Liu X, Anderson D P & Chang P R, Modification of porous starch for the adsorption of heavy metal ions from aqueous solution, *Food Chem*, 181 (2015) 133.

45 Snoeyink V L, Summers S R, *Water Supplies*, Letterman, R D, Ed, New York: Mc Graw-HillInc, (1999).
46 Wu F C, Tseng R L & Juang R S, Initial behavior of intraparticle diffusion model used in the description of adsorption kinetics, *Chem Eng J*, 153 (2009) 1.
47 Boyd G E, Adamson A W & Myers L S, The exchange adsorption of ions from aqueous solutions by organic zeolites II Kinetics, *J Am Chem Soc*, 69 (1947) 2836.
48 Foo K Y & Hameed B H, Insights into the modeling of adsorption isotherm systems, *Chem Eng J*, 156 (2010) 2.
49 Ncibi M C, Applicability of some statistical tools to predict optimum adsorption isotherm after linear and non-linear regression analysis, *J Hazard Mater*, 153 (2008) 207.
50 Hayward D O & Trapnell B M W, *Chemisorption*, London: Butterworths, (1964).
51 Reed B E & Matsumoto M R, Modeling cadmium adsorption by activated carbon using the Langmuir and Freundlich isotherm expressions, *Sep Sci Technol*, 28 (1993) 2179.
52 Swedlund P J & Webster J G, Cu and Zn ternary surface complex formation with SO_4 on ferrihydrite and schwertmannite, *Appl Geochem*, 16 (2001) 503.
53 McKay G, Otterburn M S & Sweeney A G, The removal of colour from effluent using various adsorbents-III Silica: Rate processes, *Water Res*, 14 (1980) 15.
54 Ozer A & Pirincci H B, The adsorption of Cd(II) ions on sulphuric acid-treated wheat bran, *J Hazard Mater*, B137 (2006) 849.
55 Ahmad R, Kumar R & Laskar M A, Adsorptive removal of Pb^{2+} form aqueous solution by macrocyclic calix[4]naphthalene: Kinetic, thermodynamic, and isotherm analysis, *Environ Sci Pollut Res Int*, 20 (2013) 219.